

Prenatal High-Sucrose Diet Induced Vascular Dysfunction of Renal Interlobar Arteries in the Offspring via PPAR γ -RXRg-ROS/Akt Signaling

Xueqin Feng,* Xinying Liu, Fuling Wang, Xiaoyun Zhang, Liangxi Zhu, Hua Shu, Chunxia Wang, Liting Duan, Haixia Wang, Qinggui Ren, Fangxiang Dong, Ziteng Zhang, Dongmei Man,* and Miaomiao Qu*

Scope: Prenatal nutrition imbalance correlates with developmental origin of cardiovascular diseases; however whether maternal high-sucrose diet (HS) during pregnancy causes vascular damage in renal interlobar arteries (RIA) from offspring still keeps unclear.

Methods and results: Pregnant rats are fed with normal drinking water or 20% high-sucrose solution during the whole gestational period. Swollen mitochondria and distributed myofilaments are observed in vascular smooth muscle cells of RIA exposed to prenatal HS. Maternal HS increases phenylephrine (PE)-induced vasoconstriction in the RIA from adult offspring. NG-Nitro-L-arginine (L-Name) causes obvious vascular tension in response to PE in offspring from control group, not in HS. RNA-Seq of RIA is performed to reveal that the gene retinoid X receptor g (RXRg) is significantly decreased in the HS group, which could affect vascular function via interacting with PPAR γ pathway. By preincubation of RIA with apocynin (NADPH inhibitor) or capivasertib (Akt inhibitor), the results indicate that ROS and Akt are the vital important factors to affect the vascular function of RIA exposure to prenatal HS.

Conclusion: Maternal HS during the pregnancy increases PE-mediated vasoconstriction of RIA from adult offspring, which is mainly related to the enhanced Akt and ROS regulated by the weakened PPAR γ -RXRg.

1. Introduction

The fetus under the adverse intrauterine conditions is highly susceptible to multiple adult-onset diseases in the later life, for hypertension, diabetes, and stroke.^[1-3] Recently, some researchers pointed that nutritional imbalance could lead to cardiovascular diseases.^[4-7] Notably, prenatal nutrition imbalance correlates with a greater risk of developmental origin of cardiovascular diseases.^[8-10] An ever-growing evidence base demonstrates that high sugar/sucrose diet intake may increase deaths cases and cardiovascular disease burdens.^[11,12] Therefore, much more attention should be paid to investigate the effects of high-sugar on vascular development, especially the gravida and fetus. Excessive consumption of sugar during the pregnant period could induce metabolic diseases and microvascular dysfunction in the adult offspring.^[13,14] Our previous study revealed that maternal

X. Feng, X. Liu, F. Wang, X. Zhang, L. Zhu, H. Shu, C. Wang, L. Duan, H. Wang, F. Dong, D. Man, M. Qu
Department of Obstetrics
Affiliated Hospital of Jining Medical University
Guhuai Road 89, Jining 272001, China
E-mail: fengxueqin4443@126.com; mandongmei@163.com; mm1923@163.com

X. Liu
Department of Clinical Medicine
Jining Medical University
Jining 272001, China
Q. Ren
Department of Mammary gland Surgery
Affiliated Hospital of Jining Medical University
Jining 272001, China
Z. Zhang
Departments of Thoracic Surgery
Qinghai Red Cross Hospital
Xining 272001, China

The ORCID identification number(s) for the author(s) of this article can be found under <https://doi.org/10.1002/mnfr.202300871>

© 2024 The Authors. Molecular Nutrition & Food Research published by Wiley-VCH GmbH. This is an open access article under the terms of the Creative Commons Attribution-NonCommercial-NoDerivs License, which permits use and distribution in any medium, provided the original work is properly cited, the use is non-commercial and no modifications or adaptations are made.

DOI: 10.1002/mnfr.202300871

high-sucrose diet altered vascular contraction in the offspring.^[10,15,16] However, there has limited information on underlying mechanisms to interpret the association of prenatal high-sucrose diet with vascular diseases in renal interlobar arteries from the offspring.

Renal vascular systems play an important role in vascular volume regulation and blood pressure maintenance.^[17–19] Revascularization of the interlobar renal arteries could lead to a high risk of cardiovascular diseases by disrupting vascular structure and function.^[20] Adverse factors during maternal pregnancy could induce renal reprogramming and vascular dysfunction in the offspring.^[21] However, information on whether and how vascular develops in the interlobar renal arteries of offspring exposed to prenatal high-sucrose diet is still limited. Thus, present study aims to discuss the effects of maternal high-sucrose diet during the pregnancy on the function of interlobar renal arteries from the adult offspring. The data gained would further understand the physiological and pathological characteristics of renal vessels in developmental origins.

2. Experimental Section

2.1. Animals

Four-month old Sprague–Dawley rats were purchased from Peng Yue Experimental Animal Breeding Company. They were free access to water and standard food, and housed in a controlled environment of 25 °C under a 12 light–dark cycle with cycles of air ventilation. After 1 week of recovery of transportation, one female rat was mated with two male rats. The day vaginal plugs were detected was regarded as the first day of gestation. All pregnant rats ($n = 25$ each group) were randomly divided into the control group (CON) and high-sucrose group (HS). Pregnant rats in CON were provided with standard food and tap water, and the HS group was fed with the same food and 20% sucrose solution from gestational day 1–21.^[10,13–16] Caesarean delivery was conducted on pregnant rats at gestational day 21, and the fetal kidneys were obtained immediately. Other pregnant rats were vaginal delivery naturally. Male offspring were sacrificed at 16 weeks old with a freshly prepared sodium pentobarbital (50 mg kg⁻¹) to isolate renal interlobar arteries (RIA) for testing. Body weight and kidney weight were determined at the same time. For all experiments, the pups used in present study were from different litters. All experiments were conducted in accordance with the guidelines for the Care and Use of Laboratory Animals (NIH Publication No.85–23, 1996). Ethical approval was granted by the Ethical Committee of the Affiliated Hospital of Jining Medical University (No: 2020B010).

2.2. Dosage Information/Dosage Regimen

The pregnancy rats in HS group were provided with standard food and free access to 20% w/v sucrose solution during the gestational period (GD1–GD20). According to the daily drinking volume of rats, it was equivalent to approximately 62.90 g sugar per kg per day for human.

2.3. Hematoxylin and Eosin (HE) Staining

The RIA was isolated and immediately fixed in 4% paraformaldehyde at 4 °C as described.^[10] In brief, RIA was cut into 5-mm sections and rehydrated with xylene and a descending alcohol. After washing with distilled water, the sections were stained with hematoxylin solution and eosin-phloxlike B solution. Imaging was carried out by Olympus BX53 biological microscope. After calibrating the software, the vessel wall thickness and diameter were measured. The images were analyzed with Image J software and GraphPad Prism 9 (GraphPad, San Diego, CA, USA).

2.4. Transmission Electron Microscopy

The RIA from adult offspring was fixed in 2.5% glutaraldehyde (pH = 7.4) for 2 h. After washed three times with 0.1 M phosphate buffer (pH = 7.2), the vessels were fixed again in 1% osmic acid at 4 °C for 2 h. Then, the samples were gradient dehydrated with ascending concentrations of ethanol. Subsequently, the RIA was subjected to resin penetration and embedded in epon. After position, the ultrathin section was made and counterstained with 3% uranyl acetate and 2.7% lead citrate. Finally, the sections were observed with a HT7800 transmission electron microscope.

2.5. Measurement of Vessel Tone

The RIA was cut into 3.0 mm in length and recorded with multimyograph system (Danish Myo Technology, Denmark). The organ chamber was filled with 5 mL PSS solution (mmol L⁻¹: NaCl, 120.9; NaHCO₃, 25.0; KCl, 4.7; MgSO₄·7H₂O, 1.7; CaCl₂·2H₂O, 2.8; EDTA, 0.025; KH₂PO₄, 1.2; and glucose, 5.0; 4 °C, pH = 7.4), continuously gassed with 95% O₂–5% CO₂. Each vessel ring was tested only once in this study. KCl (120 mmol)-mediated vascular contraction was regarded as contraction normalization. After equilibration for 1 h, cumulative doses (10⁻⁹ to 10⁻⁴ mol L⁻¹) of phenylephrine (PE) was used to test vascular tension. NG-Nitro-L-arginine (L-Name, endothelial nitric oxide-synthase inhibitor; 100 μmol), capivasertib (antagonist for Akt; 10 μmol), or apocynin (antagonist for NADPH oxidases-Nox; 100 μmol) were used for pretreating segments for 30 min respectively before application of PE. Signals were recorded with Power-Lab system with Chart 9 software (AD Instruments, USA) for analysis.

2.6. RNA-Seq

RNA-Seq could be used to identify and quantify all mRNA species and many noncoding RNA species. Therefore, RNA-Seq of the RIA was performed to search for differential gene sets with assistance from Shandong Jieluoxuan Biotechnology Co., Ltd. (Shandong, China). Magnetic beads with Oligo (dT) were used for RNA enrichment and purification. The rRNA was removed by kit as instruction described (Agilent Technologies, CA, USA). In brief, fragmentation buffer was added into the purified mRNA to shorten the fragments. The first strand of cDNA was synthe-

Table 1. Primer sequences in this study.

Gene	Forward primer (5'-3')	Reverse primer (3'-5')
<i>Nox1</i>	TTTTCAGTTTGCCTTTGCT	TCCAAGAGCTGAAGCAGGTT
<i>Nox2</i>	TCTTCAGCCATTCACACCAT	CAGAGAAGGGAGGCTCACCC
<i>Nox4</i>	CGGGGTGGCTTGTGAAGTAT	CCTCCAGGCAAAGATCCATG
<i>PPARα</i>	GTCCTCTGTTGTCCCTTG	TGGGGAGAGAGGACAGATGG
<i>PPARδ</i>	AGATGAGGACAACCCACGG	TGGCTGTTCCATGACTGACC
<i>PPARγ</i>	TAAGGGACTCGAGGAGGTCA	CGAAGTTGGTGGCCAGAAT
<i>RXRγ</i>	AGGCAAGAAGAGTAGAAGCGG	GCTTCCGTCAACTTGGGCTA
<i>Akt</i>	TCAGGTGCTGAGGAGATGGA	CTTGCAACGATGACCTCCT
<i>β-actin</i>	CCGCCCTAGGCACAGGGTG	GGCTGGGGTGTGAAGGTCTCAA

sized by using random primers. The 2nd strand marking buffer and 2nd strand/end repair enzyme mix were added to synthesize the 2nd strand of cDNA. Following the terminal repair, base A and sequencing joint were added. Sequentially, the target fragment was recovered by magnetic bead screening, and PCR amplification was performed to complete the whole library preparation. After the library was constructed, Qubit 3.0 was used for initial quantification and the library was diluted to 1 ng μL^{-1} , followed by Agilent 2100. Once the insert size met expectation, Q-PCR was performed using Bio-Rad CFX 96 fluorescence quantitative PCR instrument and Bio-Rad kit iQ SYBR GRN. The effective concentration of the library was quantified accurately (effective concentration >10 nM) to ensure the quality. Qualified library was sequenced on a high-throughput sequencing platform.

2.7. Real-Time PCR

Total RNA of RIA was extracted using RNA-easy Isolation Reagent (Vazyme, USA) following the manufacturer's instructions. The RNA concentration and purity were confirmed by spectrophotometer (Thermo, USA). First-strand cDNA was synthesized by HiScript III RT SuperMix for qPCR (+gDNA wiper). Real-time PCR was performed in 20 μL system including 10 μL of ChamQ Universal SYBR qPCR Master Mix, 0.4 μL of forward primer (10 μM), 0.4 μL of reverse primer (10 μM), 2 μL cDNA, and 7.2 μL of nuclease-free water, and was carried out using MyiQ2 Thermal Cycler Real-Time PCR Detection System (Bio-Rad, USA) according to the following program: one cycle at 95 $^{\circ}\text{C}$ for 30 s; 40 cycles of 10 s at 95 $^{\circ}\text{C}$, and 30 s at 60 $^{\circ}\text{C}$; one cycle at 95 $^{\circ}\text{C}$ for 15 s, 60 $^{\circ}\text{C}$ for 60 s, and 95 $^{\circ}\text{C}$ for 15 s. Expressions of genes were normalized to β -actin. The gene primer sequences were shown in Table 1.

2.8. Western Blotting

The RIA was homogenized in liquid nitrogen and lysed in RIPA buffer (Beyotime Biotech, China) containing protease inhibitors and phosphatase inhibitors (Biotool, China) to obtain the whole cell protein. Samples with equal total proteins were separated by 10% polyacrylamide gel and transferred onto polyvinylidene fluoride membranes. Following blocking nonspecific binding sites by 5% skim milk, the PVDF membranes were incubated with the

primary antibodies, including GAPDH (1:1000; Affinity, China), β -actin (1:5000; Affinity, China), RXR γ (1:1000; Affinity, China), and Akt (1:1000; Affinity, China). After the primary antibodies removed, the membrane was incubated with HRP-coupled goat antirabbit secondary antibody (1:5000; Proteintech, China) for 1 h at room temperature. Blots were visualized using enhanced chemiluminescence detection reagents (Thermo Fisher, Australia), and were recorded using an Imaging System (Tanon, Shanghai, China). Specific bands were quantified using Image J software.

2.9. Statistical Analysis

All data were presented as mean \pm SEM, and analyzed with unpaired *t*-test or two-way ANOVA followed by Bonferroni, where appropriate. The data were performed and curve fitted with GraphPad Prism 9 (GraphPad, San Diego, CA, USA). Statistical significance was defined as $p < 0.05$.

3. Results

3.1. Kidney and Body Weight

Though the fetal weight exposure to prenatal HS was high as reported,^[15] the kidney weight and the kidney weight/body weight of fetal rat were lower in the HS group (Figure 1A,B), indicating that maternal HS during the pregnancy may affect fetal kidney development. For adult offspring, no significant difference was observed in the kidney weight/body weight between CON and HS groups while the kidney weight in the HS group was significantly decreased (Figure 1C,D). The above results prompted that prenatal HS could induce renal alteration in the offspring.

3.2. HE Stains and Transmission Electron Microscopy

The RIA acted the vital important role in blood pressure maintenance.^[22,23] Vascular gross morphology was assessed with HE stains. In terms of morphometric parameters, there was no difference in the vessel wall thickness and vessel diameter between the two groups (Figure 2A).

The microstructure of RIA was further observed by transmission electron microscopy. Compared with the CON group, we found the mitochondrial injury with the higher mitochondrial area in the HS offspring characterized by mitochondrial swelling and disappearance of mitochondrial cristae in vascular smooth muscle cells of RIA. Notably, myofilament was widely, yet heterogeneously, distributed in the HS group (Figure 2B).

3.3. The Effect of Prenatal HS on PE-Induced Vascular Contractions of RIA

Vascular function was further determined in the present study. There was no significant difference in KCl-induced max

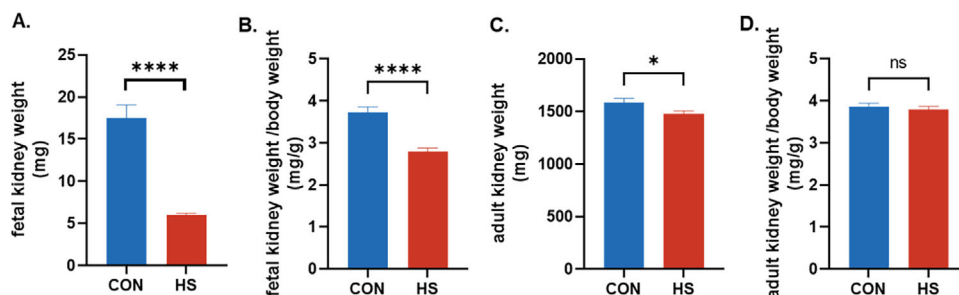


Figure 1. The effect of prenatal HS on kidney weight. A) Fetal kidney weight. B) Fetal kidney weight/body weight. *n* represents number of pregnancy from each group. C) Adult kidney weight. D) Adult kidney weight/body weight. CON: *n* = 5, HS: *n* = 5. *n* represents number of pregnancy (A, B) or offspring from different litters (C, D) of each group. Data were shown as mean ± SEM and analyzed by unpaired two-tailed Student's *t*-test. **p* < 0.05, *****p* < 0.0001.

vasoconstrictions between the two groups (Figure 3A), so KCl-induced max tension was regarded as a contractile reference. Cumulative phenylephrine (PE, 10^{-9} – 10^{-4} mol L⁻¹) was used to test the vascular response. PE produced dose-dependent contraction in RIA in both the CON and HS groups. Concentration response curve of PE-induced vascular tension in HS group was significantly greater than that in the CON group (Figure 3B). The vascular sensitivity was expressed as pD₂ (–logEC₅₀) and pD₂ values of PE-induced vasoconstrictions were significantly higher in RIA from HS adult offspring (CON: 5.68 ± 0.11 vs HS: 6.26 ± 0.25 ; *p* < 0.05, Figure 3C). There was a significant difference in response to PE in CON offspring in the absence or presence of L-Name, while not in HS group (Figure 3D,E). The data suggested that prenatal HS increased vascular tension and contraction sensitivity, which was related to endothelial dysfunction in RIA from offspring.

3.4. RNA-seq Analyses of RIA

To further clarify why vascular contractile function changes in HS group, the RIA was collected for transcriptome sequencing. Differentially expressed genes (DEGs) ($|\log_2(\text{fold change})| > 2$ and *Q*-value < 0.05) in RIA were performed with Gene Ontology (GO) classification. Of the 18 300 genes was identified, 142 genes were significantly different between CON and HS groups, and were shown in heatmap. We found that the gene retinoid X receptor *g* (RXR_g) in the RIA was significantly decreased in HS group (fold of change = 21.79% vs CON) (Figure 4A), and was confirmed by mRNA and protein detection (Figure 4B,C). In addition, Kyoto Encyclopedia of Genes and Genomes (KEGG) pathway enrichment analyses indicated that PPAR signaling had the high enrichment score (Figure 4D). The mRNA expressions of three subunits PPAR α , PPAR δ , and

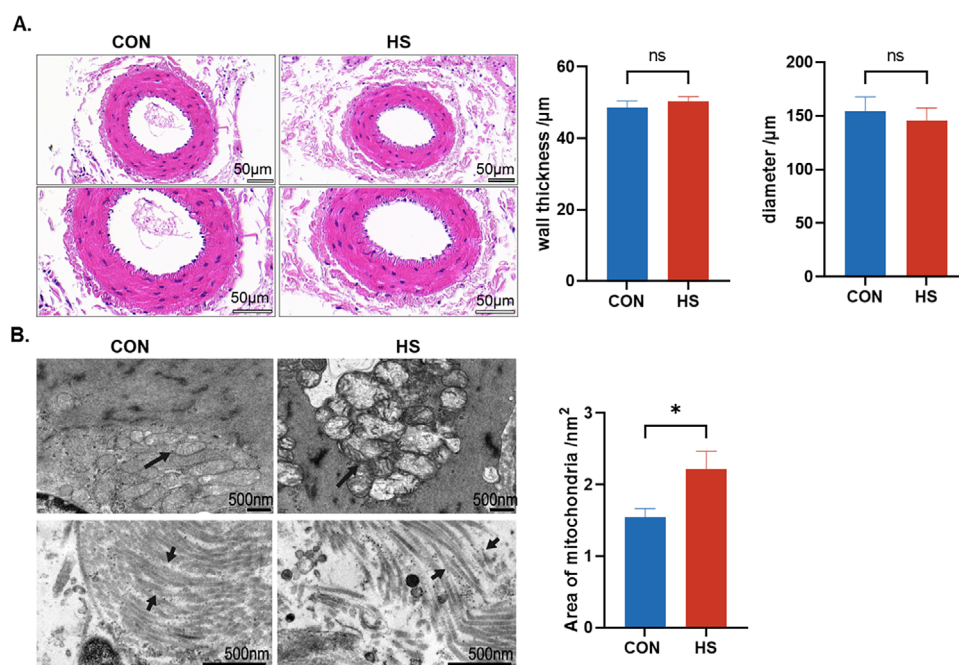


Figure 2. HE staining and transmission electron microscopy of RIA. A) HE staining of RIA. Bar: 50 µm. B) Transmission electron microscopy of RIA. Bar: 500 nm. Arrow indicated the mitochondria or myofilament arrangement. Arrows indicated mitochondria and myofilaments. CON: *n* = 3, HS: *n* = 3. *n* represents number of offspring each group. Data were shown as mean ± SEM and analyzed by unpaired two-tailed Student's *t*-test. **p* < 0.05.

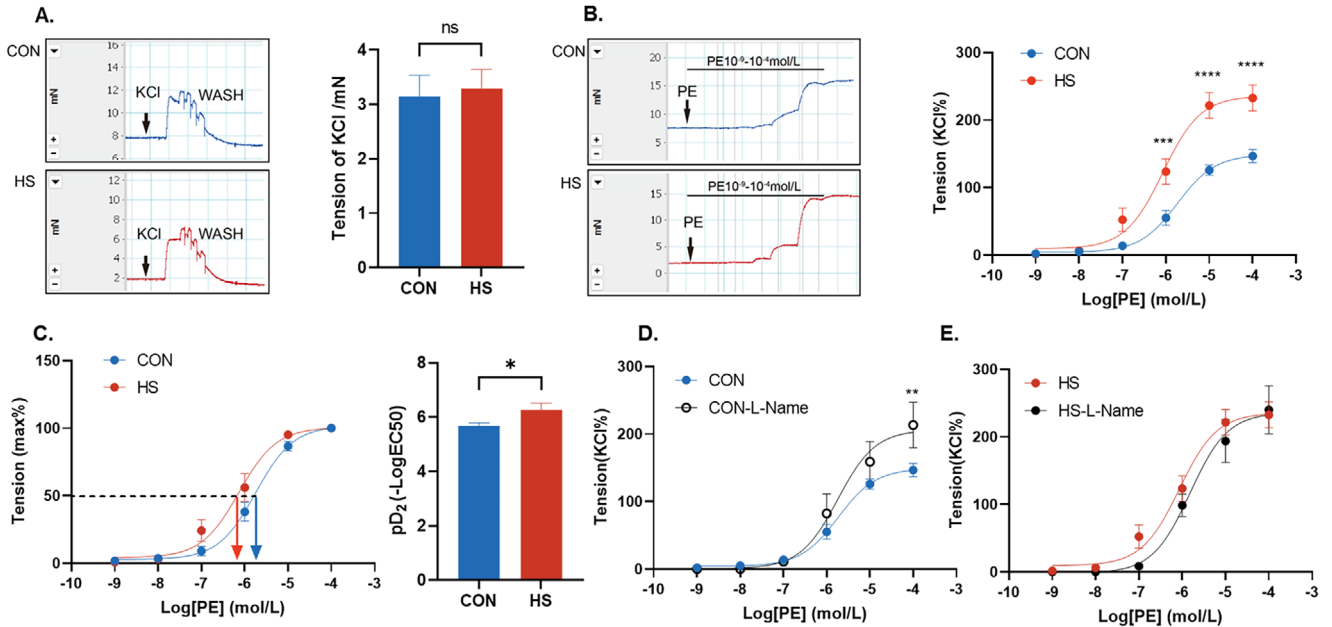


Figure 3. The effect of prenatal HS on PE-induced vascular responses of RIA. A) KCl-mediated contraction curves in RIA. B) PE-mediated contraction in RIA. C) PE-mediated contraction sensitivity expressed as pD₂ (-LogEC₅₀) in RIA. D–E) PE-mediated contraction in RIA in the absence or presence of L-Name from CON and HS groups. CON: n = 10, HS: n = 10. n represents number of offspring from different litters of each group. Data were shown as mean ± SEM and analyzed by unpaired two-tailed Student's *t*-test or two-way ANOVA followed by Bonferroni posttests. **p* < 0.05, ***p* < 0.01, ****p* < 0.001, *****p* < 0.0001.

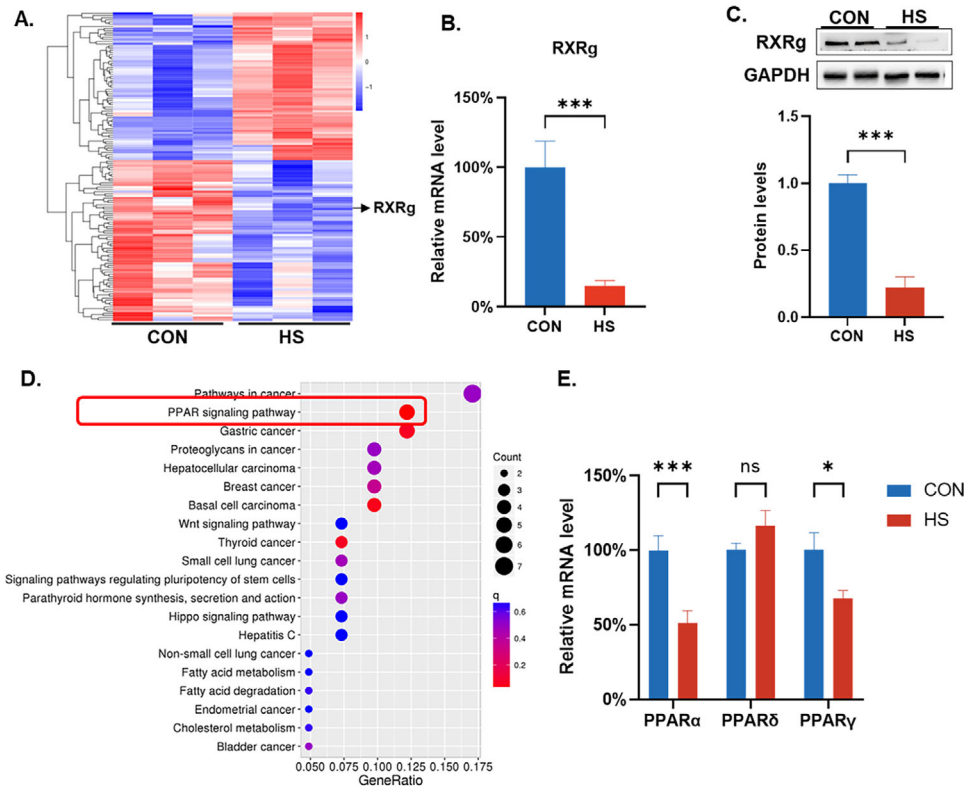


Figure 4. The RNA-seq analysis of RIA. A) Heat map of RNA-Sequence. CON: n = 3, HS: n = 3. B) The mRNA of RXRg. CON: n = 9, HS: n = 8. C) The protein expression of RXRg. CON: n = 4, HS: n = 4. D) KEGG pathway enrichment analyses. CON: n = 3, HS: n = 3. E) The mRNAs of PPAR α , PPAR δ , and PPAR γ . CON: n = 7, HS: n = 7. n represents number of offspring from different litters of each group. Data were shown as mean ± SEM and analyzed by unpaired two-tailed Student's *t*-test. **p* < 0.05, ****p* < 0.001.

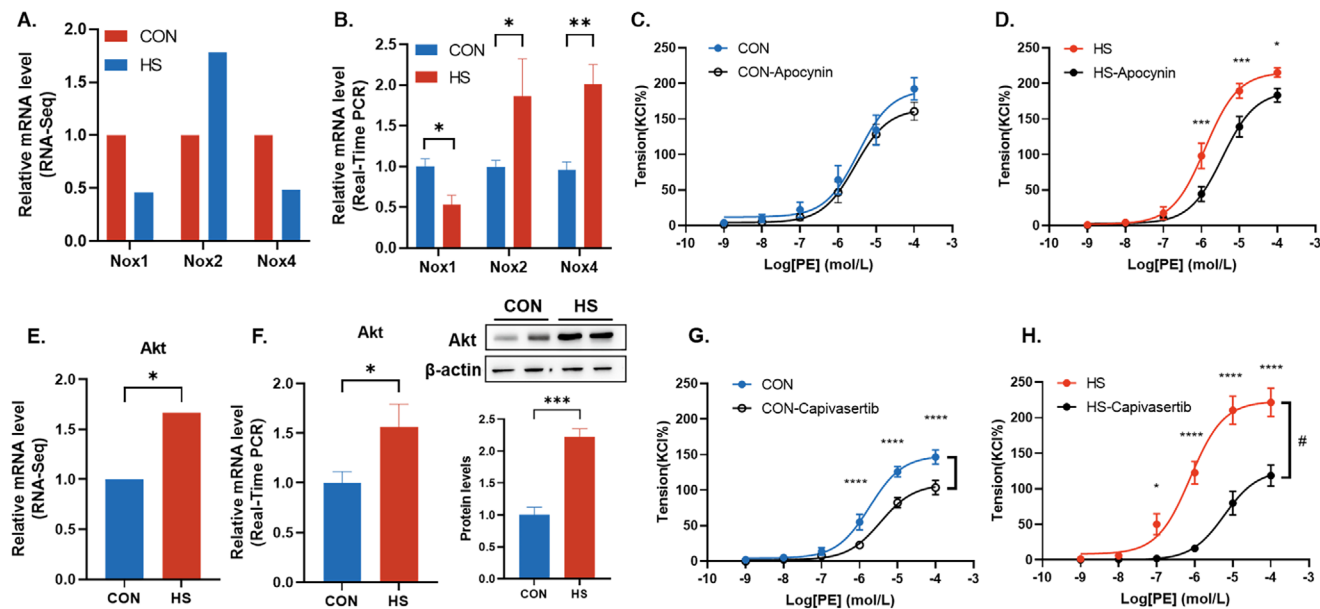


Figure 5. The roles of ROS/Akt in PE-induced vascular responses of RIA. A) The mRNA levels of Nox1, Nox2, and Nox4 detected by RNA-Seq. B) The mRNA levels of Nox1, Nox2, and Nox4 detected by real-time PCR. CON: $n = 5$, HS: $n = 5$. C–D) PE-induced contraction with or without apocynin from CON and HS group. E) The mRNA level of Akt detected by RNA-Seq. F) The mRNA and protein expression of Akt. CON: $n = 4$, HS: $n = 4$. G–H) PE-induced contraction with or without capivasertib from CON and HS group. CON: $n = 8$, HS: $n = 8$. n represents number of offspring from different litters of each group. Data were shown as mean \pm SEM and analyzed by unpaired two-tailed Student's t -test or two-way ANOVA followed by Bonferroni posttests. *, # $p < 0.05$, ** $p < 0.01$, *** $p < 0.001$, **** $p < 0.0001$.

PPAR γ were further detected as shown in Figure 4E. Previous study reported that the interactions of RXRg and activated PPAR γ played a vital role in cardiovascular disorders by regulating genes transcription.^[24–26]

3.5. The Roles of ROS and Akt in Vascular Dysfunction of RIA

PPAR γ plays a pivotal role in endothelial function by regulating gene expression. Its interaction with RXRg and the subsequent effect on ROS/Akt signaling can alter vascular reactivity, which we discuss in the context of our findings on RIA. ROS, including the superoxide anion (O_2^-), would induce oxidative stress.^[15] NADPH oxidases (Nox) are main source of O_2^- generation in the vasculature.^[27] Among the Nox family, there were Nox1, Nox2, and Nox4, mainly expressed in the vascular smooth muscle cells. Therefore, we analyzed the key genes in the pathways. As shown in Figure 5A, compared with CON, the relative mRNA levels of Nox1, Nox2, and Nox4 in RNA-Seq were changed with fold of change = 0.46, 1.79, and 0.48, respectively. Meanwhile, the mRNA levels performed by real-time PCR showed that the Nox1 was downregulated while Nox2 and Nox4 were upregulated in HS group (Figure 5B). The information suggested that prenatal HS induced the imbalance of ROS. Apocynin could inhibit Nox activity in preventing superoxide production. Between the presence and absence of apocynin, PE induced vasoconstriction showed no significant difference in CON, while that was decreased in HS group (Figure 5C,D), indicating that apocynin could partly reverse vascular function of RIA exposure to prenatal HS.

Notably, Akt kinase could mediate microvascular dysfunction by regulating endothelial nitric oxide synthase (eNOS), and also played a critical role in many important cellular processes.^[28,29] The relative mRNA level of Akt in HS detected by RNA-Seq with fold of change = 1.67 (Figure 5E), similar to the mRNA and protein expressions respectively detected by real-time PCR and western blot (Figure 5F). Capivasertib, as the Akt inhibitor, significantly inhibited PE-induced vascular tension in both CON and HS groups (Figure 5G,H). Importantly, capivasertib-decreased amplitude in HS was significantly higher than that in CON, prompting that prenatal HS significantly enhanced the Akt function.

4. Discussion

As a modern healthcare problem, high-sucrose diet, especially during the pregnancy, has been associated with increased risk of cardiovascular diseases in later life. We employed rat models to reveal the effects of prenatal high-sucrose on the function of renal interlobar arteries from adult offspring and clarify its underlying mechanisms. The main results of this experiment were as follows: 1) cumulative PE-mediated vasoconstriction was enhanced in RIA from adult offspring exposure to prenatal HS; 2) the RNA-seq analyses of RIA suggested that RXRg was significantly decreased in HS group, and KEGG pathway enrichment analyses indicated that RXRg could interact with PPAR pathways to affect vascular endothelial function; 3) vascular hypocontractility induced by PE in HS group could be inhibited by apocynin and capivasertib, indicating that both abundant ROS and Akt signaling participated in regulating vascular dysfunction. Together, the present study demonstrated that prenatal high-sucrose had

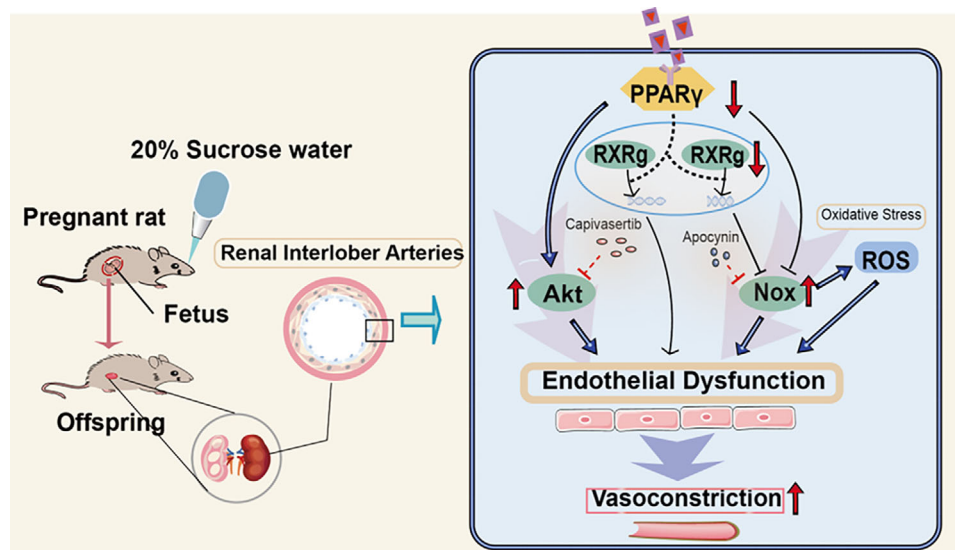


Figure 6. Summarized image of vascular hypo-contractility in RIA from offspring exposure to prenatal HS. Prenatal high-sucrose diet increased phenylephrine (PE)-mediated vasoconstriction of renal interlobar arteries (RIA) from offspring. Maternal high-sucrose diet enhanced ROS and Akt signaling, which could be regulated by the weakened PPAR γ -RXR γ , leading to vascular dysfunction in offspring.

significant influence on vascular function in renal arteries from offspring. Together, the data gained offered new information to further understand the characteristics of renal vessels in developmental origins. **Figure 6** summarized the working model.

Previous study pointed that adverse factors during pregnancy could cause poor renal development in offspring.^[21] In this study, prenatal HS decreased the kidney weight in both the fetus and adult offspring, suggesting that high-sucrose diet during pregnancy has affected kidney development later. However, the lower kidney weight/body-weight ratio was found in fetus, not in adult offspring, which may be caused by “catch-up growth” after birth. Additionally, the swollen mitochondria and distributed myofilament were observed in vascular smooth muscle cells of RIA exposed to prenatal HS, indicating that antenatal high-sucrose diet has an effect on the vascular structure alteration. Histological microstructure is the basis for vascular function. Whether RIA can be functionally affected by prenatal factors is the important focus of the present study. Importantly, we firstly confirmed that the vascular responses and LogEC50 induced by cumulative PE were significantly enhanced in the RIA exposure to prenatal HS. The higher vascular tension and sensitivity may result in vascular diseases in RIA from the HS offspring. The finding about functional changes following prenatal exposure to high-sucrose diet offered new information on prenatal nutrition imbalance-affected development in kidney vascular systems. Endothelial function corrects with vascular tension. Therefore, nitric oxide mediation of endothelium dependent relaxation was evaluated using L-Name in the present study. L-Name significantly potentiated PE-mediated vasoconstrictions only in CON group, not in HS group. The information suggested that the increased tension in HS group may be closely related to endothelial dysfunction.

However, the underlying mechanism of vascular dysfunction exposed to prenatal high-sucrose diet still keeps unclear. Thus, we collected RIA for RNA-Seq. The GO analyses demonstrated that the gene RXR γ was significantly decreased in HS group

that was confirmed by mRNA and protein detection. In addition, KEGG pathway enrichment analyses indicated that PPAR signaling had the high enrichment score. The PPAR family consists of PPAR α , PPAR γ and PPAR δ .^[30] PPAR γ is expressed in all components of the vascular system including endothelial cells, vascular smooth muscle cells, and monocytes/macrophages.^[31,32] Notably, activation of PPAR γ was reported to increase endothelial nitric oxide synthase activity and improve the left ventricular remodeling of infarcted hearts.^[33] Previous study reported that the interactions of activated PPAR γ and RXR γ played a vital role in cardiovascular disorders by regulating genes transcription.^[24–26] Both transcriptional sequencing and RT-PCR results showed that the expressions of PPAR γ and RXR γ were decreased in present study, indicating that PPAR γ -RXR γ was involved in the regulation of RIA in offspring exposure to prenatal high-sucrose diet. The mechanisms mediating vascular dysfunction involve endothelial dysfunction, smooth muscle contraction attenuation, and inhibition of proliferation and inflammation.^[34] As a ligand-dependent nuclear receptor, PPAR γ plays an important role in kidney physiology and contribute to arterial blood pressure regulation and hypertension development by modulating other signaling pathways,^[35] including the ROS and Akt pathways, all of which are reported to associated with high blood pressure.^[36] Therefore, we further characterized the roles of the downstream ROS signal and Akt signal in the RIA regulations in the present study.

Intracellular ROS has been linked to the occurrence of chronic adult diseases such as hypertension, atherosclerosis, and diabetes.^[37] It is generally agreed that elevated vascular ROS triggers an atherosclerotic process by mediating proinflammatory signaling activation and endothelial dysfunction.^[38] As the major source of ROS in the vasculature, Noxs are the key players in mediating redox signaling under physiological and pathophysiological conditions.^[39] As the members of the Nox family, Nox1, Nox2, and Nox4 are predominantly expressed in vascular

smooth cell.^[40] Recent study pointed that overproduction of ROS induced endothelial dysfunction from micro vessel under condition of high glucose.^[41,42] Consistent with the transcriptome sequencing analysis, the mRNA expression of Nox2 and Nox4 determined by RT-PCR was significantly increased in RIA from the HS group, which might result in abnormal ROS levels in RIA in HS offspring. As a natural compound, apocynin has been widely used as a Nox inhibitor in animal models of ROS-related diseases, for cardiovascular, metabolic, liver, and neurodegenerative diseases.^[43–45] In this study, PE-induced vascular dysfunction by excessive ROS in HS could be partially restored by Nox inhibitor apocynin, indicating that prenatal HS-enhanced vascular contractions in the offspring were involved in abnormal ROS production.

The Akt signaling is also an intracellular signal transduction pathway that is involved in many cells process, including cell metabolism, proliferation, survival, and angiogenesis.^[46] Previous study indicated that activation of PPAR γ could inhibit Akt signaling pathway, thus, to prevent vascular remodeling.^[47] Moreover, PPAR γ could phosphorylate Akt via mediating other signaling pathways implicating kinases.^[35,48] Present data showed that high-sucrose diet during pregnancy indeed increased the mRNA and protein expression of Akt in interlobar renal artery tissues in HS group. And preincubation with the Akt inhibitor-capivasertib decreased vascular constriction, and the capivasertib-sensitive curve in HS group was greater than the CON group, which suggested that the function of Akt was enhanced in the RIA from HS offspring.

Vascular endothelium plays an essential role in modulating vascular tone, and unhealthy endothelium would lead to hypertension and other cardiovascular risk factors. We have showed that prenatal HS diet damaged vascular endothelial function of RIA from adult offspring with L-Name. It is known to all that both abnormal ROS and Akt signals could mediate vascular endothelial dysfunction through both direct and indirect processes,^[49,50] although we have not further verified it in present study. All evidences in the present study prompted that the combined action of abnormal ROS and enhanced Akt disrupted endothelial function of RIA exposure to maternal high-sucrose diet during the pregnancy.

In conclusion, this study revealed that antenatal high-sucrose diet increased PE-mediated vasoconstrictions in renal interlobar arteries of the offspring, and this phenomenon may due to the endothelial dysfunction mediated by ROS and Akt pathway via abnormal PPAR γ -RXR γ regulation. The new data obtained provided crucial information on understanding of pathological characteristics of RIA following exposure to antenatal high-sucrose diet and represented a novel therapeutic approach to prevent the onset of endothelium-related diseases.

Acknowledgements

This work was supported by the National Nature and Science Foundation of China (82101797), the Natural Science Foundation of Shandong Province (ZR2021QH131), Key Research and Development Program of Jining Science (2023YXNS030), PhD Research Foundation of Affiliated Hospital of Jining Medical University (2021-BS-025) and Central Guiding Local Science and Technology Development Fund Project (No. 2023ZY002).

Conflict of Interest

The authors declare no conflict of interest.

Author Contributions

X.F. and X.L. contributed equally to this work and share first authorship. X.Q.F. conceptualized the research. X.Y.L. conducted the experiment, and wrote the draft. X.Q.F. revised the paper. X.Q.F., D.M.M., and M.M.Q. had the primary responsibility for final content. Other authors listed have made a direct and substantial contribution to animal feeding or sample preparation. All authors read and approved it for publication.

Data Availability Statement

The original contributions presented in the study are included in the article material. Further inquiries can be directed to the corresponding authors.

Keywords

Akt, RIA, ROS, RRAR γ , vasoconstriction

Received: December 7, 2023

Revised: March 21, 2024

Published online:

- [1] T. Xu, B. Ji, L. Li, J. Lei, M. Zhao, M. Sun, Z. Xu, Q. Gao, *Hypertension* **2022**, *79*, 1997.
- [2] Q. Zheng, Y. He, L. Li, C. Rui, N. Li, Y. Zhang, Y. Ye, Z. Zhang, X. Yang, J. Tang, Z. Xu, *Nutrients* **2023**, *15*, 245.
- [3] J. Lei, M. Zhao, F. Deng, T. Xu, B. Ji, X. Wang, M. Zhang, M. Sun, Q. Gao, *J. Mol. Cell. Cardiol.* **2023**, *181*, 46.
- [4] G. B. D. A. Collaborators, *Lancet Public Health* **2023**, *8*, 585.
- [5] V. W. Zhong, D. Yu, L. Zhao, Y. Yang, X. Li, Y. Li, Y. Huang, G. Ding, H. Wang, *Ann. Intern. Med.* **2023**, *176*, 1037.
- [6] T. O. E. de Crom, L. Blekkenhorst, M. W. Vernooij, M. K. Ikram, T. Voortman, M. A. Ikram, *Am. J. Clin. Nutr.* **2023**, *118*, 352.
- [7] R. Balasubramanian, K. H. Shutta, M. Guasch-Ferre, T. Huang, S. C. Jha, Y. Zhu, A. H. Shadyab, J. E. Manson, D. Corella, M. Fito, F. B. Hu, K. M. Rexrode, C. B. Clish, S. E. Hankinson, L. D. Kubzansky, *Brain Behav. Immun.* **2023**, *114*, 262.
- [8] Y. Liu, C. Yang, X. Feng, L. Qi, J. Guo, D. Zhu, P. N. Thai, Y. Zhang, P. Zhang, M. Sun, J. Lv, L. Zhang, Z. Xu, X. Lu, *Mol. Nutr. Food Res.* **2020**, *64*, 2000196.
- [9] Q. Zheng, N. Li, Y. Zhang, J. Li, E. Zhang, Z. Xu, *Mol. Nutr. Food Res.* **2023**, *67*, 2200722.
- [10] X. Feng, T. Yu, Y. Zhang, L. Li, M. Qu, J. Wang, F. Dong, L. Zhang, F. Wang, F. Zhang, X. Zhou, Z. Xu, D. Man, *Mol. Nutr. Food Res.* **2021**, *65*, 2100072.
- [11] D. D. Torricco, J. Tam, S. Fuentes, C. Gonzalez Viejo, F. R. Dunshea, *J. Sci. Food Agric.* **2020**, *100*, 3024.
- [12] C. E. Kearns, L. A. Schmidt, S. A. Glantz, *JAMA Intern. Med.* **2016**, *176*, 1680.
- [13] P. Zhang, D. Zhu, Y. Zhang, L. Li, X. Chen, W. Zhang, R. Shi, J. Tao, B. Han, Z. Xu, *Mol. Nutr. Food Res.* **2018**, *62*, 1700771.
- [14] A. He, Y. Zhang, Y. Yang, L. Li, X. Feng, B. Wei, D. Zhu, Y. Liu, L. Wu, L. Zhang, Z. Xu, M. Sun, *Brain Res.* **2017**, *1669*, 114.
- [15] X. Feng, X. Zhou, W. Zhang, X. Li, A. He, B. Liu, R. Shi, L. Wu, J. Wu, D. Zhu, N. Li, M. Sun, Z. Xu, *Biol. Reprod.* **2017**, *96*, 1085.
- [16] X. Feng, X. Li, C. Yang, Q. Ren, W. Zhang, N. Li, M. Zhang, B. Zhang, L. Zhang, X. Zhou, Z. Xu, *Mol. Nutr. Food Res.* **2019**, *63*, 1900022.

- [17] T. H. Mohamed, H. Watanabe, R. Kaur, B. C. Belyea, P. D. Walker, R. A. Gomez, M. L. S. Sequeira-Lopez, *Hypertension* **2020**, *76*, 458.
- [18] J. Dalman, D. M. Coleman, *Surg Clin. North Am.* **2023**, *103*, 733.
- [19] O. Edosuyi, A. Adesuyi, M. Choi, I. Igbe, A. Oyekan, *Eur. J. Pharmacol.* **2023**, *938*, 175441.
- [20] Y. Ding, C. C. Wu, V. Garcia, I. Dimitrova, A. Weidenhammer, G. Joseph, F. Zhang, V. L. Manthati, J. R. Falck, J. H. Capdevila, M. L. Schwartzman, *Am. J. Physiol. Renal. Physiol.* **2013**, *305*, 753.
- [21] L. Jiang, X. Yin, A. He, L. Li, L. Bo, X. Zhou, J. Tang, X. Gu, J. Wu, Q. Gao, J. Lv, C. Mao, Z. Xu, *J. Nutr. Biochem.* **2016**, *28*, 121.
- [22] J. Tang, Z. Zhu, S. Xia, N. Li, N. Chen, Q. Gao, L. Li, X. Zhou, D. Li, X. Zhu, Q. Tu, W. Li, C. Wu, J. Li, Y. Zhong, X. Li, C. Mao, Z. Xu, *Sci. Rep.* **2015**, *5*, 9723.
- [23] E. L. Schiffrin, *Am. J. Hypertens.* **2004**, *17*, 1192.
- [24] T. M. De Silva, M. L. Modrick, P. Ketsawatsomkron, C. Lynch, Y. Chu, C. J. Pelham, C. D. Sigmund, F. M. Faraci, *Hypertension* **2014**, *64*, 1088.
- [25] F. Azam, M. Bello, *Molecules* **2022**, *27*, 5778.
- [26] T. S. Hughes, P. K. Giri, I. M. de Vera, D. P. Marciano, D. S. Kuruvilla, Y. Shin, A. L. Blayo, T. M. Kamenecka, T. P. Burris, P. R. Griffin, D. J. Kojetin, *Nat. Commun.* **2014**, *5*, 3571.
- [27] B. Lassegue, D. Sorescu, K. Szocs, Q. Yin, M. Akers, Y. Zhang, S. L. Grant, J. D. Lambeth, K. K. Griendling, *Circ. Res.* **2001**, *88*, 888.
- [28] G. Song, G. Ouyang, S. Bao, *J. Cell. Mol. Med.* **2005**, *9*, 59.
- [29] X. Lu, J. Yao, C. Li, L. Cui, Y. Liu, X. Liu, G. Wang, J. Dong, Q. Deng, Y. Hu, D. Guo, W. Wang, C. Li, *Front. Pharmacol.* **2022**, *13*, 840521.
- [30] B. Grygiel-Gorniak, *Nutr. J.* **2014**, *13*, 17.
- [31] O. Braissant, F. Fougelle, C. Scotto, M. Dauca, W. Wahli, *Endocrinology* **1996**, *137*, 354.
- [32] R. E. Law, S. Goetze, X. P. Xi, S. Jackson, Y. Kawano, L. Demer, M. C. Fishbein, W. P. Meehan, W. A. Hsueh, *Circulation* **2000**, *101*, 1311.
- [33] N. Kobayashi, T. Ohno, K. Yoshida, H. Fukushima, Y. Mamada, M. Nomura, H. Hirata, Y. Machida, M. Shinoda, N. Suzuki, H. Matsuoka, *Am. J. Hypertens.* **2008**, *21*, 576.
- [34] J. Plutzky, *Circ. Res.* **2011**, *108*, 1002.
- [35] M. Kvandova, M. Barancik, P. Balis, A. Puzserova, M. Majzunova, I. Dovinova, *J. Physiol. Pharmacol.* **2018**, *69*, 231.
- [36] C. M. Halabi, A. M. Beyer, W. J. de Lange, H. L. Keen, G. L. Baumbach, F. M. Faraci, C. D. Sigmund, *Cell Metab.* **2008**, *7*, 215.
- [37] C. Kunsch, R. M. Medford, *Circ. Res.* **1999**, *85*, 753.
- [38] R. S. Frey, M. Ushio-Fukai, A. B. Malik, *Antioxid. Redox Signal.* **2009**, *11*, 791.
- [39] H. Morawietz, *Basic Res. Cardiol.* **2011**, *106*, 521.
- [40] K. Schroder, M. Zhang, S. Benkhoff, A. Mieth, R. Pliquett, J. Kosowski, C. Kruse, P. Luedike, U. R. Michaelis, N. Weissmann, S. Dimmeler, A. M. Shah, R. P. Brandes, *Circ. Res.* **2012**, *110*, 1217.
- [41] J. Goldney, J. A. Sargeant, M. J. Davies, *Diabetologia* **2023**, *66*, 1832.
- [42] Z. Zhang, X. Li, J. He, S. Wang, J. Wang, J. Liu, Y. Wang, *J. Thromb. Thrombolysis* **2023**, *56*, 388.
- [43] M. S. Petronio, M. L. Zeraik, L. M. Fonseca, V. F. Ximenes, *Molecules* **2013**, *18*, 2821.
- [44] S. H. Lee, B. Y. Choi, A. R. Kho, J. H. Jeong, D. K. Hong, D. H. Kang, B. S. Kang, H. K. Song, H. C. Choi, S. W. Suh, *Int. J. Mol. Sci.* **2018**, *19*, 3087.
- [45] T. Munzel, G. G. Camici, C. Maack, N. R. Bonetti, V. Fuster, J. C. Kovacic, *J. Am. Coll. Cardiol.* **2017**, *70*, 212.
- [46] I. Hers, E. E. Vincent, J. M. Tavare, *Cell Signal.* **2011**, *23*, 1515.
- [47] T. Hussain, L. Chai, Y. Wang, Q. Zhang, J. Wang, W. Shi, Q. Wang, M. Li, X. Xie, *Heliyon.* **2023**, *9*, e14173.
- [48] A. Janaszak-Jasiecka, A. Ploska, J. M. Wieronska, L. W. Dobrucki, L. Kalinowski, *Cell. Mol. Biol. Lett.* **2023**, *28*, 21.
- [49] K. Yang, S. Velagapudi, A. Akhmedov, S. Kraler, T. Lapikova-Bryhinska, M. O. Schmiady, X. Wu, L. Geng, G. G. Camici, A. Xu, T. F. Luscher, *Cardiovasc. Res.* **2023**, *119*, 2190.
- [50] C. L. Busceti, A. Carrizzo, F. Bianchi, M. De Lucia, A. Damato, C. Cazzin, E. Venturini, P. Di Pietro, R. P. Ginerete, L. Di Menna, M. Cotugno, R. Stanzione, S. Marchitti, S. Migliarino, M. Ciccarelli, S. Sciarretta, V. Bruno, G. Battaglia, F. Fornai, M. Volpe, S. Rubattu, F. Nicoletti, C. Vecchione, *Circ. Res.* **2023**, *132*, 1489.